ГИАБ. Горный информационно-аналитический бюллетень /
MIAB. Mining Informational and Analytical Bulletin, 2023;(4):20-34
ОРИГИНАЛЬНАЯ СТАТЬЯ / ORIGINAL PAPER

УДК 622.831; 624.121.54 DOI: 10.25018/0236_1493_2023_4_0_20

МЕТОДИКА ПРОГНОЗА НАПРЯЖЕННО-ДЕФОРМИРОВАННОГО СОСТОЯНИЯ МЕЖДУКАМЕРНЫХ ЦЕЛИКОВ, ЗАКРЕПЛЕННЫХ ПОДАТЛИВОЙ ТРОСОВОЙ КРЕПЬЮ

А.А. Беликов[1], Н.А. Беляков[1]

[1] Санкт-Петербургский горный университет, Санкт-Петербург, Россия, e-mail: s205046@stud.spmi.ru

Аннотация: Представлен способ податливого крепления междукамерных целиков в породах, склонных к проявлению реологических свойств. Разработана методика прогноза деформаций закрепленных целиков на примере системы разработки десятой западной панели по пласту АБ на Верхнекамском месторождении калийно-магниевых солей. Численная реализация модели выполнена методом конечных элементов в программном комплексе Simulia Abaqus с использованием вязко-упруго-пластической геомеханической модели сильвинита. Параметрическое обеспечение реологической модели выполнено на основе результатов инструментальных наблюдений за деформациями междукамерных целиков. Прогноз выполнялся на срок в 150 лет после проходки камер. Установлено, что величина горизонтального смещения боковой поверхности незакрепленных междукамерных целиков равна 123 мм за период прогноза. Произведен сравнительный анализ работы тросовой крепи при различных диаметрах канатов и величинах реакций крепи в податливом режиме работы. Выявлен экспоненциальный характер зависимости продолжительности податливого и жесткого режимов работы крепи и критерия эффективной ее работы. Из представленных данных видно, что увеличение эффективности работы крепи возрастает при использовании каната большего диаметра, однако выбор максимального диаметра каната ограничивается конструктивными особенностями крепи. Приведено уравнение зависимости горизонтальных смещений боковой поверхности закрепленного целика от времени и реакции крепи. Прогноз напряженно-деформированного состояния закрепленных целиков показал положительный эффект податливой крепи по увеличению несущей способности целика как во время ее работы, так и после ее разрушения.

Ключевые слова: устойчивость, междукамерный целик, податливая крепь, способ податливого крепления целиков, тросовая крепь, соляные породы, ползучесть, водозащитная толща.

Для цитирования: *Беликов А. А., Беляков Н. А.* Методика прогноза напряженно-деформированного состояния междукамерных целиков, закрепленных податливой тросовой крепью // Горный информационно-аналитический бюллетень. – 2023. – № 4. – С. 20–34. DOI: 10.25018/0236_1493_2023_4_0_20.

Method of predicting the stress-strain state of interchamber pillars lined with a compliant rope fastener

A.A. Belikov[1], N.A. Belyakov[1]

[1] Saint-Petersburg Mining University, Saint-Petersburg, Russia, e-mail: s205046@stud.spmi.ru

Abstract: The method of compliant fixing of inter-compartment pillars in the rocks prone to the exhibiting of rheological properties is presented in this article. The method of forecasting the deformations of anchored pillars is developed using the example of the development system of the tenth western panel of the AB formation, Verkhnekamskoe deposit of potassium-magnesium salts. Numerical realization of the model is performed by the finite element method in the software package Simulia Abaqus with the use of visco-elastic-plastic geomechanical model of sylvinite. Parametric support for the rheological model was made on the basis of the results of measurements of horizontal displacements of contour benchmarks interchamber pillars. The forecast was carried out for a period of 150 years after the chambers were fully developed. It has been established that the value of horizontal displacement of lateral surface of unlined interchamber pillars is equal to 123 mm for the forecast period. A comparative analysis of wire rope fastening operation with different rope diameters and fastener reaction values in the undercut mode of operation has been carried out. The exponential character of dependence between the duration of underlay and rigid regime of the roof support and the criterion of its effective work was revealed. It is evident from the presented data that the increase of the fastener efficiency increases with the use of a larger diameter rope, but the choice of the maximum rope diameter is limited by the design features of the fastener. The equation of dependence of horizontal displacements of the side surface of the anchored pillar on time and fastener reaction is given in the work. The forecast of the stress-strain state of the anchored pillars showed a positive effect of the supple support to increase the bearing capacity of the pillar both during its operation and after its destruction.

Key words: stability, interchamber pillar, compliant fastener, method of compliant fastening of pillars, rope fastener, salt rock, creep, water-protective strata.

For citation: Belikov A. A., Belyakov N. A. Method of predicting the stress-strain state of interchamber pillars lined with a compliant rope fastener. *MIAB. Mining Inf. Anal. Bull.* 2023;(4):20-34. [In Russ]. DOI: 10.25018/0236_1493_2023_4_0_20.

Introduction

Rheological properties of salt rocks play a key role in predicting the stability of inter-chamber pillars. Under the influence of stresses, both time-independent elastic deformations and time-dependent creep deformations appear in them [1, 2]. In works [3, 4] the necessity of applying measures to preserve bearing capacity of inter-chamber pillars at salt deposits is shown. In some cases, deformation of inter-chamber pillars may lead to occurrence of hydraulically connected system of cracks in water-protective strata (WPS) [5—7]. Water breakthrough into the mined-out space of water-soluble ores can lead to an avalanche-like accident at the plant, followed by the formation of karst sinkholes on the surface [8—10]. In practice, hydrofilling of the mined-out space is used as measures to ensure the integrity of the WPS [11]. Such measures do not take into account the rheological nature of the deformation of inter-chamber pillars, the backfill does not provide sufficient resistance to the transverse deformation of inter-chamber pillars in salt formations [12, 13].

The operational period of the mine is about 50 years, and the realization of the subsidence of the surface after full excavation — 100 years, which leads to a long period of subsidence of the ground surface

and the emergence of hydraulically connected system of cracks in the WPS [1, 14]. A compliant support in salt rocks was considered in [15—17], where its positive effect due to the decrease of rheological processes intensity is noted. The monitoring of changes in the stress-strain state (STS) of the anchored section of the bulk is a time-consuming and sometimes dangerous task. In this regard, the rheological prediction of stress-strain state makes it possible to select the support parameters on the basis of given parameters of deformation [17, 18].

The purpose of this work is to develop a method of forecasting deformations of inter-chamber pillars secured by compliant cable lining.

Key stages of numerical modelling

Prediction of geomechanical processes occurring in interchamber pillars and in the vicinity of chambers was performed in Simulia Abaqus software package by finite element method [12, 16, 19]. Forecast was carried out for a period of 150 years after sinking of chambers. The numerical model was made in the 2D plane deformation formulation with discretization of the considered area into quadrangular elements of the second order. Fig. 1 shows the computational scheme reflecting parameters of the development system of the tenth western panel in the AB formation at the SKRU-1 mine at an average depth of 366 m. The model includes overlying rock pressure and boundary conditions: the lateral faces of the model are constrained to move horizontally and the lower face is constrained to move vertically.

The use of the visco-elastic-plastic model of sylvinite behavior is caused by geomechanical processes in the salt rocks of inter-chamber pillars, which occur in a time perspective [4, 20]. Deformation of inter-chamber pillars is determined by both stress value and strength, deformation and rheological properties of rocks. Instantaneous strength and strain properties of rocks prone to rheological properties are determined by analyzing the diagrams of total deformation of rock samples [1, 21]. It is known that in saline rocks, the strain modulus value nonlinearly decreases with increasing load on the sample [22]. In the sylvinite model, this dependence of deformation properties is obtained from the results of laboratory tests described in [23] (Fig. 2, *a*) and is tabulated. On the diagram of complete deformation, the fol-

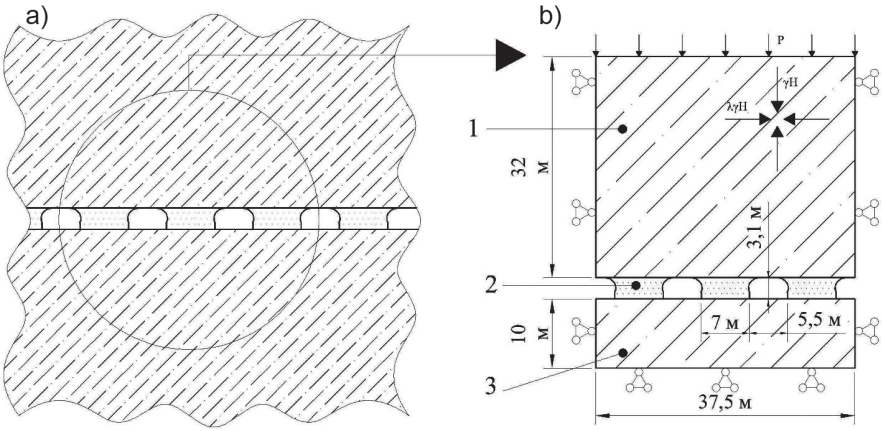

1 — WPS rocks, 2 — inter-chamber pillar, 3 — rocks of productive strata

Fig. 1. Calculation scheme: section along the panel section (a); modeled area (b)

Рис. 1. Расчетная схема: разрез по участку панели (а); моделируемая область (б)

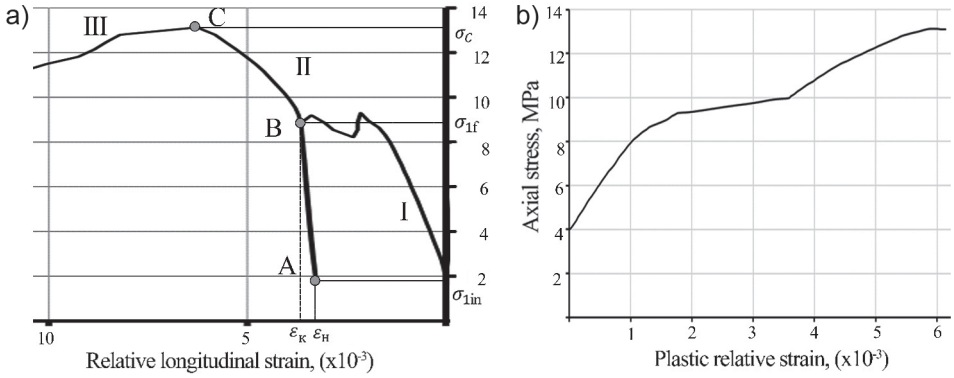

Fig. 2. Analysis of the deformation diagrams of sylvinite samples: diagram of the total deformation of the rock (a); diagram of the plastic hardening of the rock (b)

Рис. 2. Анализ диаграммы деформирования образцов сильвинита: диаграмма полного деформирования породы (а); диаграмма пластического упрочнения породы (б)

lowing sections can be distinguished: I — linear section of elastic behavior of the rock under loading; II — section of inelastic behavior of the rock, accumulation of plastic deformations and plastic hardening of the sample; III — prohibitive branch — process of destruction of the sample with stress decay; segment AB — section corresponding to unloading of the rock sample to determine the value of elastic deformations. The angle of slope of the segment AB determines the modulus of elasticity of the rock. The final ε_f and initial ε_{in} relative longitudinal strains for a given range of loading during unloading (σ_{1f} — σ_{1in}) determine the value of elastic strains. The plastic hardening diagram (Fig. 2, *b*) is obtained by subtracting the elastic strain value from the total strain diagram. At stresses higher than σ_c, the rock sample fails.

Since in the presented work only interchamber pillars and their anchoring are considered in detail, to model the mechanical behavior of the host rocks, it is acceptable to use the geomechanical model of a linearly deformed body eliminating unnecessary complication of the model [3, 24, 25]. To describe the behavior of salt rocks, we used the Drucker-Prager model, where the rate of relative creep deformation depends on the equivalent creep stress according to (1). The model is based on the notion that isosurfaces of creep stress points exist which have the same «intensity» of creep as measured by the equivalent creep stress (σ_{cr}). The model combines visco-elastic-plastic deformations of the material; a schematic representation of the rheological model is shown in Fig. 3, *a*. The material is plasticized over an equivalent creep surface, which coincides with the yield surface [20, 26, 27]. Selection of model parameters was based on the results of instrumental observations made at underground observation stations located in workings along the AB formation in the tenth western panel at the SKRU-1 mine. In the course of measurements, which lasted more than five years, horizontal displacements of contour benchmarks in the opposite walls of the chambers — on the surfaces of interchamber pillars were determined. Fig. 3 shows a graph of horizontal displacements of the pillar surface in the presented rheological model and results of instrumental observations averaged over the panel [23].

$$\dot{\varepsilon}_{cr} = \left(A(\sigma_{cr})^n \left[(m+1)\varepsilon_{cr} \right]^m \right)^{\frac{1}{m+1}}, \quad (1)$$

where $\dot{\varepsilon}_{cr}$ — the rate of relative creep deformation; σ_{cr} — equivalent creep stress;

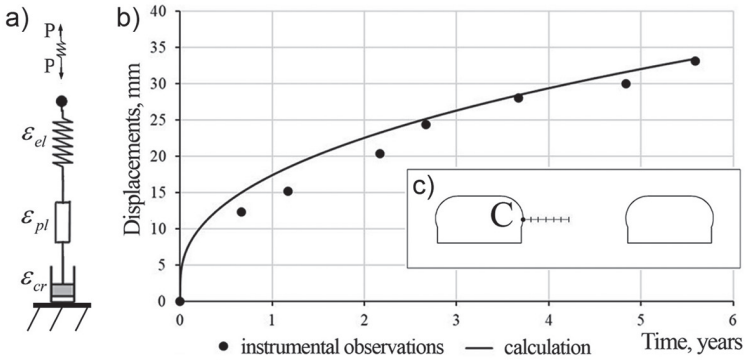

ε_{el}, ε_{pl}, ε_{cr} – elastic, plastic and viscous deformations, respectively; *C* – contour reference point

Fig. 3. Verification of the rheological model of sylvinite: schematic representation of the Drucker-Prager rheological model (a); horizontal displacements of the side surface of the target (b); layout of reference points of the measuring station (c)

Рис. 3. Верификация реологической модели сильвинита: схематическое представление реологической модели Друкера-Прагера (а); горизонтальные смещения боковой поверхности целика (б); схема расположения реперов замерной станции (в)

ε_{cr} — creep deformation value; *A*, *m*, *n* — material creep parameters set as functions of temperature and stress state.

From Fig. 3, *b* show that the simulation results showed good qualitative correspondence between the calculated and measured displacements of the contour benchmarks. It can be concluded that the parameters of the salt rock model correctly reflect the rheological character of deformation of inter-chamber pillars under the conditions in question [20, 28]. The instantaneous strength and strain properties of salt rocks in the massif are determined by the results of laboratory tests, since there is no scale effect. The rheological properties of salt rocks directly depend on the duration of the load, and the results of modeling such properties depend on the geometric dimensions of the model [29]. A such approach to the prediction of the stress-strain state of rocks prone to the manifestation of rheological properties is widely used in practice [1, 15, 16, 23]. The values of the physical and mechanical properties of gangue in the model are taken as average for the deposit [1, 3]. Physical and mechanical properties of rocks are presented in Table 1.

Supple wire rope support (RF patent No. 2788185) is installed on inter-chamber pillars in order to increase their carrying capacity by creating resistance to the cross deformation of pillars. The support arises due to the tension of ropes, the ends of which are put through the drilled holes. The rope is fixed that there is a node of suppression on the surface of the pillar in the excavation, and the tension of the rope is transmitted to reinforcing rods installed horizontally on opposite sides on the sur-

Table 1

Physical and mechanical properties of rocks
Физико-механические свойства пород

Name	Density, kg/m³	Elastic modulus, MPa	Poisson's ratio	Angle of internal friction, °	Creep constants		
					A	*n*	*m*
Sylvinite	2500	200	0,35	40	$1.9 \cdot 10^{-10}$	1	–0,59
Gangue	2500	400	0,32	51	—		

face of the pillar. The described construction works as a «coupler» with the possibility to determine the response of the fastener in the suppression mode and the magnitude of the suppression, as well as the bearing capacity. Pre-tensioning of the rope is created in the process of fastening the underflexion knot, it provides compression of all fastener elements and momentary inclusion of it in the work. The response of the fastener in the underrun mode depends on the adjustment of the underrun knot. The value of the compliance is equal to the length of the clamped rope loop in the compliance node. The carrying capacity of a roof support is limited by the carrying capacity of the rope. Fig. 4 shows the design of inter-chamber pillar anchorage tier.

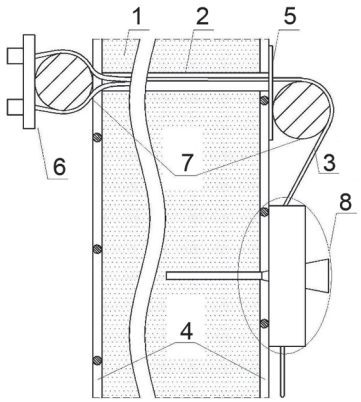

1 – pillar; 2 – target; 3 – steel rope;
4 – reinforcement mesh; 5 – support slab;
6 – load-bearing support slab;
7 – reinforcement bar; 8 – suppression node

Fig. 4. Design of the anchoring tier
Рис. 4. Конструкция яруса крепления

The anchorage works in the following way. Loaded interchamber pillars are deformed over time, expanding [30 — 32], which leads to an increase in rope tension. When a given force is reached, the fastening compression is realized by slippage of the rope in the compression node. As the suppleness is exhausted, the rate of growth of transverse deformations and stresses in the pillar is damped. When the compliance is exhausted, the load is fully transferred to the ropes — the shoring works rigidly: as the rope tension increases, the shoring back pressure increases. When the load on the shoring exceeds it's carrying capacity, the ropes plastically deform and rupture, which is accompanied by the disappearance of the support of the shoring. A typical graph of stress change in the rope and a schematic representation of the corresponding deformation of the anchored pillar are shown in Fig. 5. The section of change in the rate of stress increase in the rope shows the occurrence of plastic deformations. The duration of underlay operation is determined by the magnitude of underlay and the rate of deformation of the pillar at the corresponding pillar backing [15, 16, 33]. The strength of the steel rope, which depends on its cross-section and steel properties [34, 35], has the greatest influence on the duration of the hard mode of fastener operation and limits the maximum value of the fastener reaction in the underrunning mode. The choice of the maximum diameter of the rope is limited by the design features of the fastener: the passage of both ends of the rope through the well, and the wrapping of the rope loop around the reinforcing bar.

For a comparative analysis of the fastening work with different rope diameters and values of fastening reactions in a compliant mode of operation four versions of ropes with a diameter of 5.6, 12, 16.5 and 22.5 mm according to GOST 2688-80 and three values of fastening reactions in a compliant mode of operation 40, 60 and 80 kN for a rope diameter of 12 mm and five — 40, 60, 80, 120 and 160 kN for a rope diameter of 16.5 mm are considered in this work. The values of the rope reactions for the 5.6 and 22.5 mm ropes will correspond to their breaking tension, namely 19.3 and 303.5 kN. These variants are given for analysis of obtained results and for

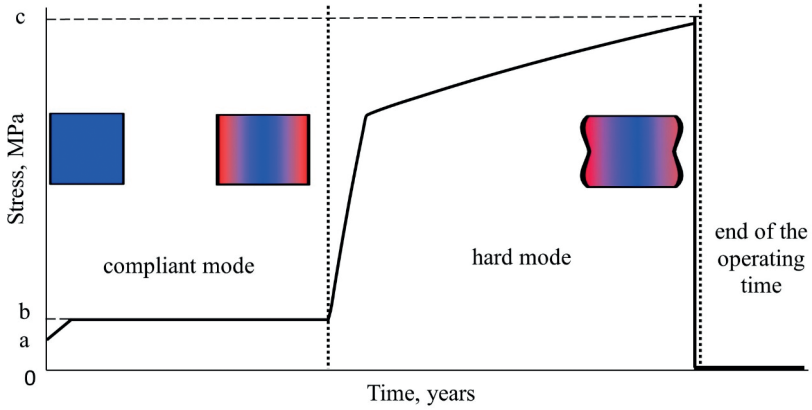

Fig. 5. Characteristic graph of the change in axial stresses in a steel wire rope: pre-tensioning (a); fastener reaction in the suppressed mode of operation (b); breaking force of the rope (c)

Рис. 5. Характерный график изменения осевых напряжений в стальном канате: предварительное натяжение (а); реакция крепи в податливом режиме работы (б); разрывное усилие каната (в)

revealing of regularities in development of the deflected stress of anchored inter-chamber pillars. Characteristics of support elements accepted for the calculation: wire rope is made of steel grade 50 with yield point 330 MPa; reinforcement mesh, made of steel grade A500 with diameter of longitudinal and transverse reinforcement of 16 mm and a step of 200 mm; reinforcing bar with diameter 80 mm, made of steel grade A500.

Results discussion

Based on the results of forecasting the deformations of unanchored inter-chamber pillars, the displacement value of their lateral surface equals 123 mm over 150 years (Fig. 6). The value of rock contour displacement for the pillars during the period of supple mode is assumed to be equal to half of the value of displacement of loose pillar 62 mm. Duration of rigid mode of support operation is determined from calculations.

Table 2

Duration of fastener operation
Продолжительность работы крепи

Rope diameter, mm	Fastening reaction, kN	Fastener operating time, years			Remaining time, years
		in compliant mode	in hard mode	total	
5.6	19.3	28.3	40.7	69	81
12	40	28.8	48.5	77.3	72.7
12	60	29.6	49.7	79.3	70.7
12	80	30.4	50.5	81.0	69.0
16.5	40	28.8	58.4	87.1	62.9
16.5	60	29.6	59.6	89.2	60.8
16.5	80	30.4	60.8	91.2	58.8
16.5	120	31.6	63.3	94.9	55.1
16.5	160	33.3	65.7	99	51
22.5	303.5	39.0	104.0	143.0	7.0

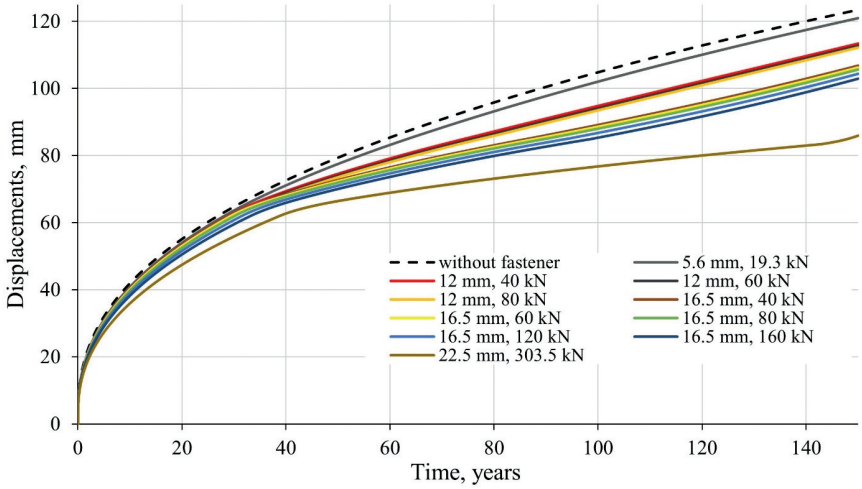

Fig. 6. Calculated horizontal displacements of the side surface of the pillar
Рис. 6. Расчетные горизонтальные смещений боковой поверхности целика

Table 2 shows duration of fastener operation and remaining forecasting time for each variant under consideration. Fig. 6 shows graphs of changes in horizontal displacements of the side surface of the pillars from time. The relative increase in the rate of pillar deformation after failure of a compliant support is clearly visible (Fig. 6) in the case with the greatest response of the support in the compliant mode of operation, which is explained by the least deformations of the pillar during the previous stages of the forecast.

Fig. 7 shows calculated horizontal displacements of pillar surface at given time intervals, corresponding to the maximum permissible values of support reactions in the suppressed mode of operation. They lie on exponential approximating curves (2), connecting which forms the surface (Fig. 8).

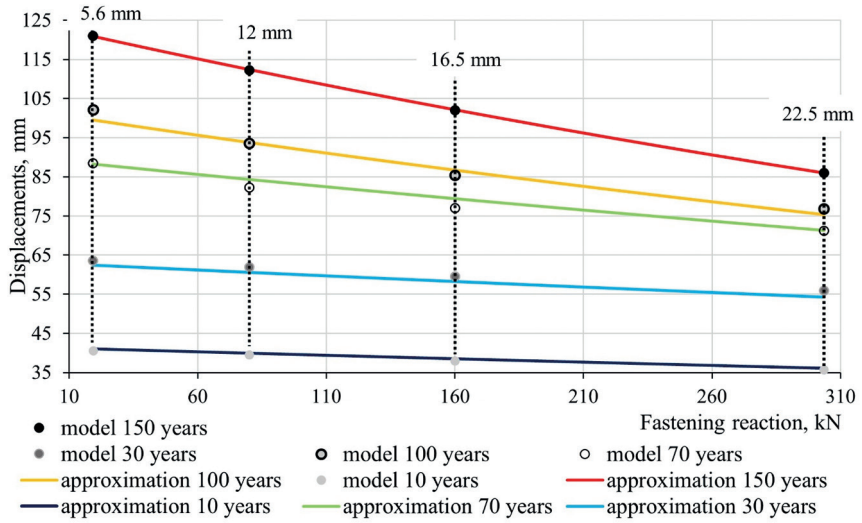

Fig. 7. Resulting values of side surface of the pillar horizontal displacements
Рис. 7. Результирующие величины горизонтальных смещений боковой поверхности целика

$$u = A(t) \cdot e^{-C(t) \cdot F}, \qquad (2)$$

where u — horizontal displacements of the side surface of the pillar at the end of the forecast period, mm; F — limit reaction of the fastener for the used rope, kN; $A(t)$, $C(t)$ — coefficients reflecting the forecast time.

Coefficients $A(t)$ и $C(t)$ are reliably approximated by a third-degree polynomial (3), (4).

$$A(t) = (3.645 \cdot 10^{-5}) \cdot t^3 - \\ -0.011 \cdot t^2 + 1.476 \cdot t + 27.736, \qquad (3)$$

$$C(t) = (-5.29 \cdot 10^{-10}) \cdot t^3 + (1.27 \cdot 10^{-7}) \cdot t^2 - \\ -(2.27 \cdot 10^{-6}) \cdot t + (4.63 \cdot 10^{-4}) \qquad (4)$$

Substituting equations (3) and (4) into (2), we obtain a surface equation characterizing the dependence of horizontal displacements of the anchored pillar lateral surface on time and fastener reaction in the compliant mode of operation (Fig. 8)

Increasing the fastener's reaction in the compliant mode leads to an increase in the duration of the compliant and hard mode of the fastener and, accordingly, to an increase in the service life of the fastener. The choice of a larger rope cross-section leads to an increase in the duration of the rigid mode of the fastener. This is explained by the condition of the hard mode of support operation. A wire rope with a larger cross-section can bear heavier loads, which increases both the back pressure and the duration of the work of the roof support. The support to the cross-sectional deformation of pillars, created at the initial stage of the service life of the pillar, affects the growth rate of cross-sectional deformations and stresses in the pillar both during the current stage and during the subsequent stages. Consequently, the most effective way to increase load-carrying capacity of the pillar would be to choose a larger cross-section rope and create maximum permissible value of pillar reaction in the compliant mode of operation.

Fig. 9 shows graphs showing the dependence of specific horizontal displacements of the rock contour of the pillar, the duration of compliant and hard mode of support operation on the diameter of the rope used. Specific horizontal displacement

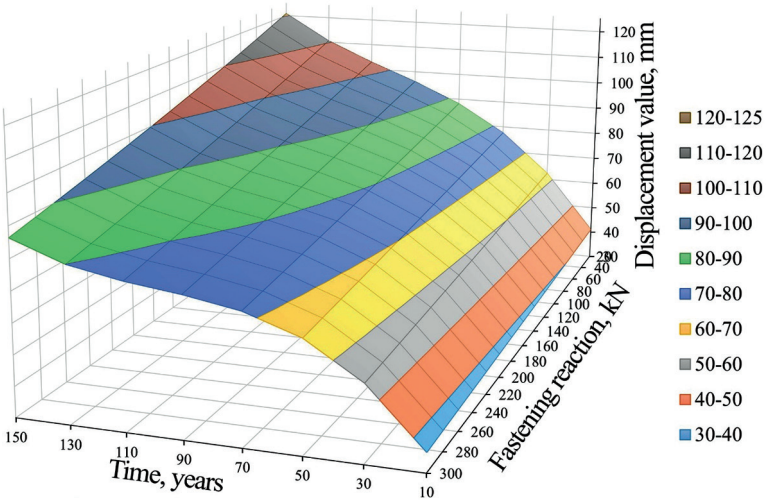

Fig. 8. Surface of horizontal displacements of the lateral surface of the lined pillar: the color indicates the displacement value

Рис. 8. Поверхность горизонтальных смещений боковой поверхности закрепленного целика: цветом обозначена величина смещения

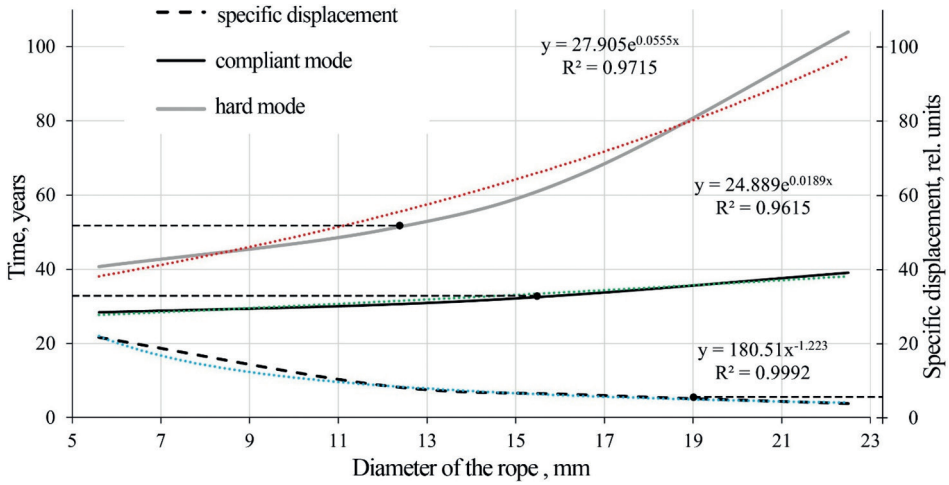

Fig. 9. Changes in the stress-strain state of the lined pillar depending on the diameter of the rope used
Рис. 9. Изменение НДС закрепленного массива в зависимости от диаметра используемого каната

of the rock contour of the pillar is the ratio of the displacement value to the diameter of the rope. The graph shows approximating exponential equations of dependence, they have a good enough convergence with the predicted data. The reduction of specific horizontal displacement of the rock contour of the pillar when selecting a larger cross-section rope indicates a more efficient operation of the roof support, but in practice the value of the maximum diameter of the rope is limited by the design features of the anchorage.

Conclusion

In this work a method of compliant anchoring of inter-chamber pillars in rocks prone to the display of rheological properties, as well as a method of predicting deformations of anchored pillars are proposed. The study considered one tier of pillar fixing, this method allows using several such tiers distributed along the height of the pillar. A comparative analysis of wire rope fastening operation at different fastener reactions in the compliant mode and rope diameters is provided.

The dependences of changes in the horizontal displacement of the rock contour on the fastening reaction in the compliant mode of operation and time are revealed. The parameters of the surface equation and its graphic representation have been obtained. The exponential character of dependences of the duration of underlay and hard mode of the roof support operation on the diameter of the rope used has been established. The analysis of the stress-strain state of the fastened massif showed an increase in the fastening efficiency at larger rope diameters — a power dependence.

Forecasting of stress-strain state of anchored pillars showed the positive effect of compliant anchorage on the increase of bearing capacity of pillar both during its operation and after its destruction. The described results indicate that the presented method of inter-chamber pillar fixing in salt formations may be used as measures to ensure the integrity of water-protective formation and to reduce losses of mineral resources in the chamber system of development. The method of predicting the integrity of water-protective strata using the described method of compliant fixing of inter-compartmental pillars is a promising area for research development.

СПИСОК ЛИТЕРАТУРЫ

1. *Кашников Ю. А.*, *Ермашов А. О.*, *Ефимов А. А.* Геолого-геомеханическая модель участка Верхнекамского калийного месторождения // Записки Горного института. — 2019. — Т. 237. — С. 259—267. DOI: 10.31897/PMI.2019.3.259.

2. *Das A. J.*, *Paul P. S.*, *Mandal P. K.*, *Kumar R.*, *Tewari S.* Investigation of failure mechanism of inclined coal pillars: Numerical modelling and tensorial statistical analysis with field validations // Rock Mechanics and Rock Engineering. 2021, vol. 54, no. 6, pp. 3263—3289.

3. *Барях А. А.*, *Губанова Е. А.* О мерах охраны калийных рудников от затопления // Записки Горного института. — 2019. — Т. 240. — С. 613—620. DOI: 10.31897/ PMI.2019.6.613.

4. *Habibi R.*, *Moomivand H.*, *Ahmadi M.*, *Asgari A.* Stability analysis of complex behavior of salt cavern subjected to cyclic loading by laboratory measurement and numerical modeling using LOCAS (case study: Nasrabad gas storage salt cavern) // Environmental Earth Sciences. 2021, vol. 80, no. 8, pp. 1—21. DOI: 10.1007/s12665-021-09620-8.

5. *Baryakh A. A.*, *Stazhevskii S. B.*, *Timofeev E. A.* Strain state of a rock mass above karst cavities // Journal of Mining Science. 2008, vol. 44, no. 6, pp. 531—538. DOI: 10.1007/s10913-008-0059-1.

6. *Куранов А. Д.*, *Багаутдинов И. И.*, *Котиков Д. А.*, *Зуев Б. Ю.* Комплексный подход к прогнозу устойчивости предохранительного целика при слоевой системе разработки запасов Яковлевского месторождения // Горный журнал. — 2020. — № 1. — С. 115—119. DOI: 10.17580/gzh.2020.01.23.

7. *Ilyukhin D.*, *Gusev V.* The use of the finite element method for ensuring efficient and safe extraction of minerals // Key Engineering Materials. 2017, vol. 743, pp. 411—416. DOI: 10.4028/www.scientific.net/KEM.743.411.

8. *Александрова Т. Н.*, *Кузнецов В. В.*, *Иванов Е. А.* Исследование влияния ионов жесткости воды на флотируемость медно-никелевых руд // Горный информационно-аналитический бюллетень. — 2022. — № 6-1. — С. 263—278. DOI: 10.25018/0236_1493_2022_61_0_263.

9. *Kiyani V.*, *Esmaili A.*, *Alijani F.*, *Samani S.*, *Vasić L.* Investigation of drainage structures in the karst aquifer system through turbidity anomaly, hydrological, geochemical and stable isotope analysis (Kiyan springs, western Iran) // Environ Earth Sciences. 2022, vol. 81, no. 22, article 517. DOI: 10.1007/s12665-022-10627-y.

10. *Мустафин М. Г.*, *Кологривко А. А.*, *Васильев Б. Ю.* Анализ точности построения цифровых моделей рельефа на основе данных периодического воздушного лазерного сканирования горнопромышленного объекта // Горный журнал. — 2023. — № 2. — С. 56—62. DOI: 10.17580/gzh.2023.02.09.

11. *Васильева М. А.*, *Волчихина А. А.*, *Морозов М. Д.* Оборудование и технологии для проведения работ по дозакладке выработанного пространства // Горный информационно-аналитический бюллетень. — 2021. — № 6. — С. 133—144. DOI: 10.25018/0236_1493_2021_6_0_133.

12. *Baryakh A. A.*, *Lobanov S. Y.*, *Lomakin I. S.* Analysis of time-to-time variation of load on interchamber pillars in mines of the Upper Kama Potash Salt Deposit // Journal of Mining Science. 2015, vol. 51, no. 4, pp. 696—706. DOI: 10.1134/S1062739115040064.

13. *Паньков И. Л.*, *Морозов И. А.* Деформирование соляных пород при объемном многоступенчатом нагружении // Записки Горного института. — 2019. — Т. 239. — С. 510—519. DOI: 10.31897/PMI.2019.5.510.

14. *Morozov K. V.* Creation of rock mass monitoring deformations systems on rock burst hazardous mineral deposits / 14th Internetional Congress on Rock Mechanics and Rock Engineering. 2020, pp. 1318–1323.

15. *Karasev M. A.*, *Protosenya A. G.*, *Katerov A. M.*, *Petrushin V. V.* Analysis of shaft lining stress state in anhydrite-rock salt transition zone // Rudarsko Geolosko Naftni Zbornik. 2022, no. 12, pp. 151–162. DOI: 10.17794/rgn.2022.1.13.

16. *Протосеня А. Г.*, *Катеров А. М.* Развитие напряженно-деформированного состояния комбинированной крепи вертикального ствола, пройденного в соляном массиве // Горный информационно-аналитический бюллетень. — 2022. — № 6-1. — С. 100—113. DOI: 10.25018/0236_1493_2022_61_0_100.

17. *Дементьева А. В.*, *Карасев М. А.* Конструкции податливых крепей в соляных породах // Горный информационно-аналитический бюллетень. — 2022. — № 10-1. — С. 136 — 144. DOI: 10.25018/0236_1493_2022_101_0_136.

18. *Shabarov A. N.*, *Kuranov A. D.*, *Kiselev V. A.* Assessing the zones of tectonic fault influence on dynamic rock pressure manifestation at Khibiny deposits of apatite-nepheline ores // Eurasian Mining. 2021. vol. 3, no. 2, pp. 3—7. DOI: 10.17580/em.2021.02.01.

19. *Гендлер С. Г.*, *Фазылов И. Р.*, *Абашин А. Н.* Результаты экспериментальных исследований теплового режима нефтяных шахт при термическом способе добычи нефти // Горный информационно-аналитический бюллетень. — 2022. — № 6-1. — С. 248—262. DOI: 10.25018/0236_1493_2022_61_0_248.

20. *Zhang Y., Xiong X., Musa M., Lyu X.* Analysis of a compressive strength model for FRP-confined damaged concrete columns based on the Drucker-Prager yield criterion // Structural Concrete. 2022, vol. 24, pp. 721—735. DOI: 10.1002/suco.202100584.

21. *Fabre G., Pellet F.* Creep and time-dependent damage in argillaceous rocks // International Journal of Rock Mechanics and Mining Sciences. 2006, vol. 43, no. 6, pp. 950—960. DOI: 10.1016/j.ijrmms.2006.02.004.

22. *Пантелеев И. А.*, *Плехов О. А.*, *Наймарк О. Б.*, *Евсеев А. В.*, *Паньков И. Л.*, *Асанов В. А.* Особенности локализации деформации при растяжении сильвинита // Вестник Пермского национального исследовательского политехнического университета. Механика. — 2015. — № 2. — С. 127—138. DOI: 10.15593/perm.mech/2015.2.08.

23. *Ермашов А. О.* Геомеханическое обоснование расчетов оседания земной поверхности при добыче калийно-магниевых руд (на примере Верхнекамского месторождения калийно-магниевых солей). Автореф. дис. ... канд. техн. наук. — Пермь: ГИ УрО РАН, 2015.

24. *Frenelus W., Peng H., Zhang J.* Creep behavior of rocks and its application to the long-term stability of deep rock tunnels // Applied Sciences. 2022, vol. 12, no. 17, article 8451. DOI: 10.3390/app12178451.

25. *Baryakh A. A.*, *Samodelkina N. A.*, *Konosavsky P. K.* Prevention of freshwater breakthrough into potassium mines // Procedia Structural Integrity. 2021, vol. 32 no. 6, pp. 17—25. DOI: 10.1016/j.prostr.2021.09.004.

26. *Zhang L., Wang X.* Study on nonlinear damage creep model for rocks under cyclic loading and unloading // Advances in Materials Science and Engineering. 2021, vol. 2021, article 5512972, pp. 1—10. DOI: 10.1155/2021/5512972.

27. *Fei W., Jie L., Quanle Z., Cunbao L., Jie C., Renbo G.* A triaxial creep model for salt rocks based on variable-order fractional derivative // Mechanics of Time-Dependent Materials. 2021, vol. 25, no. 1, pp. 101—118. DOI: 10.1007/s11043-020-09470-0.

28. *Асанов В. А.*, *Паньков И. Л.*, *Кузьминых В. С.*, *Морозов И. А.* Методические аспекты определения прочностных, деформационных и энергетических характеристик соляных пород при прямом растяжении породных образцов в лабораторных условиях // Вестник Пермского национального исследовательского политехнического университета. Механика. — 2018. — № 4. — С. 58—68. DOI: 10.15593/perm.mech/2018.4.05

29. *Протосеня А. Г.*, *Катеров А. М.* Обоснование параметров реологической модели соляного массива // Горный информационно-аналитический бюллетень. — 2023. — № 3. — С. 16—28. DOI: 10.25018/0236_1493_2023_3_0_16.

30. *Deng H., Zhou H., Li L.* Fractional creep model of temperature-stress-time coupled damage for deep coal based on temperature-equivalent stress // Results in Physics. 2022, vol. 39, article 105765, pp. 1—12. DOI: 10.1016/j.rinp.2022.105765.

31. *Taheri S. R., Pak A.* Casing failure in salt rock: Numerical investigation of its causes // Rock Mechanics and Rock Engineering. 2020, no. 59, pp. 3903 – 3918. DOI: 10.1007/s00603-020-02161-9.

32. *Кашников Ю. А., Ашихмин С. Г., Кухтинский А. Э., Шустов Д. В.* О связи коэффициентов трещиностойкости и геофизических характеристик горных пород месторождений углеводородов // Записки Горного института. – 2020. – Т. 241. – С. 83 – 90. DOI: 10.31897/PMI.2020.1.83.

33. *Moghadam S. I., Taheri E., Ahmadi M., Ghoreishian Amiri S. A.* Unified bounding surface model for monotonic and cyclic behaviour of clay and sand // Acta Geotechnica. 2022, vol. 17, no. 10, pp. 4359 – 4375. DOI: 10.1007/s11440-022-01521-9.

34. *Shammazov I., Dzhemilev E., Sidorkin D.* Improving the method of replacing the defective sections of main oil and gas pipelines using laser scanning data // Applied Sciences. 2023, vol. 13, no. 1, article 48. DOI: 10.3390/app13010048.

35. *Abdelwahab A., Chishegorov D., Ivanov S., Mikhailov A.* Influence of the main operational factors on the working capacity of a mining hydraulic excavator // E3S Web of Conferences. 2021, vol. 326, article 00007. DOI: 10.1051/e3sconf/202132600007. ГИАБ

REFERENCES

1. Kashnikov Yu. A., Ermashov A. O., Efimov A. A. Geological and geomechanical model of the section of the Verkhnekamskoye potash deposit. *Journal of Mining Institute*. 2019, vol. 237, pp. 259 – 267. [In Russ]. DOI: 10.31897/PMI.2019.3.259.

2. Das A. J., Paul P. S., Mandal P. K., Kumar R., Tewari S. Investigation of failure mechanism of inclined coal pillars: Numerical modelling and tensorial statistical analysis with field validations. *Rock Mechanics and Rock Engineering*. 2021, vol. 54, no. 6, pp. 3263 – 3289.

3. Baryakh A. A., Gubanova E. A. On measures to protect potash mines from flooding. *Journal of Mining Institute*. 2019, vol. 240, pp. 613 – 620. DOI: 10.31897/ PMI.2019.6.613.

4. Habibi R., Moomivand H., Ahmadi M., Asgari A. Stability analysis of complex behavior of salt cavern subjected to cyclic loading by laboratory measurement and numerical modeling using LOCAS (case study: Nasrabad gas storage salt cavern). *Environmental Earth Sciences*. 2021, vol. 80, no. 8, pp. 1 – 21. DOI: 10.1007/s12665-021-09620-8.

5. Baryakh A. A., Stazhevskii S. B., Timofeev E. A. Strain state of a rock mass above karst cavities. *Journal of Mining Science*. 2008, vol. 44, no. 6, pp. 531 – 538. DOI: 10.1007/s10913-008-0059-1.

6. Kuranov A. D., Bagautdinov I. I., Kotikov D. A., Zuev B. Yu. An integrated approach to predicting the stability of a safety pillar in a layered system of developing reserves of the Yakovlevskoye field. *Gornyi Zhurnal*. 2020, no. 1, pp. 115 – 119. [In Russ]. DOI: 10.17580/gzh.2020.01.23.

7. Ilyukhin D., Gusev. V. The use of the finite element method for ensuring efficient and safe extraction of minerals. *Key Engineering Materials*. 2017, vol. 743, pp. 411 – 416. DOI: 10.4028/www.scientific.net/KEM.743.411.

8. Aleksandrova T. N., Kuznetsov V. V., Ivanov E. A. Investigation of the water hardness ions impact on the copper-nickel ores flotation probability. *MIAB. Mining Inf. Anal. Bull.* 2022, no. 6-1, pp. 263 – 278. [In Russ]. DOI: 10.25018/0236_1493_2022_61_0_263.

9. Kiyani V., Esmaili A., Alijani F., Samani S., Vasić L. Investigation of drainage structures in the karst aquifer system through turbidity anomaly, hydrological, geochemical and stable isotope analysis (Kiyan springs, western Iran). *Environ Earth Sciences*. 2022, vol. 81, no. 22, article 517. DOI: 10.1007/s12665-022-10627-y.

10. Mustafin M. G., Kologrivko A. A., Vasiliev B. Yu. Analysis of the accuracy of building digital terrestrial models based on periodic airborne laser scanning of a mining object. *Gornyi Zhurnal*. 2023, no. 2, pp. 56 – 62. [In Russ]. DOI: 10.17580/gzh.2023.02.09.

11. Vasilyeva M. A., Volchikhina A. A., Morozov M. D. Re-backfill technology and equipment. *MIAB. Mining Inf. Anal. Bull.* 2021, no. 6, pp. 133—144. [In Russ]. DOI: 10.25018/0236_1493_2021_6_0_133.

12. Baryakh A. A., Lobanov S. Y., Lomakin I. S. Analysis of time-to-time variation of load on interchamber pillars in mines of the Upper Kama Potash Salt Deposit. *Journal of Mining Science*. 2015, vol. 51, no. 4, pp. 696—706. DOI: 10.1134/S1062739115040064.

13. Pankov I. L., Morozov I. A. Salt Rock Deformation under bulk multiple-stage loading. *Journal of Mining Institute*. 2019, vol. 239, pp. 510—519. [In Russ]. DOI: 10.31897/PMI.2019.5.510.

14. Morozov K. V. Creation of rock mass monitoring deformations systems on rock burst hazardous mineral deposits. *14th Internetional Congress on Rock Mechanics and Rock Engineering*. 2020, pp. 1318–1323.

15. Karasev M. A., Protosenya A. G., Katerov A. M., Petrushin V. V. Analysis of shaft lining stress state in anhydrite-rock salt transition zone. *Rudarsko Geolosko Naftni Zbornik*. 2022, no. 12, pp. 151–162. DOI: 10.17794/rgn.2022.1.13.

16. Protosenya A. G., Katerov A. M. Development of stress and strain state of combined support for a vertical shaft driven in salt massif. *MIAB. Mining Inf. Anal. Bull.* 2022, no. 6-1, pp. 100—113. [In Russ]. DOI: 10.25018/0236_1493_2022_61_0_100.

17. Dementyeva A. V., Karasev M. A. Design of yielding support systems in salts. *MIAB. Mining Inf. Anal. Bull.* 2022, no. 10-1, pp. 136 — 144. [In Russ]. DOI: 10.25018/0236_1493_2022_101_0_136.

18. Shabarov A. N., Kuranov A. D., Kiselev V. A. Assessing the zones of tectonic fault influence on dynamic rock pressure manifestation at Khibiny deposits of apatite-nepheline ores. *Eurasian Mining*. 2021. vol. 3, no. 2, pp. 3—7. DOI: 10.17580/em.2021.02.01.

19. Gendler S. G., Fazylov I. R., Abashin A. N. The results of experimental studies of the thermal regime of oil mines in the thermal method of oil production. *MIAB. Mining Inf. Anal. Bull.* 2022, no. 6-1, pp. 248—262. [In Russ]. DOI: 10.25018/0236_1493_2022_61_0_248.

20. Zhang Y., Xiong X., Musa M., Lyu X. Analysis of a compressive strength model for FRP-confined damaged concrete columns based on the Drucker-Prager yield criterion. *Structural Concrete*. 2022, vol. 24, pp. 721—735. DOI: 10.1002/suco.202100584.

21. Fabre G., Pellet F. Creep and time-dependent damage in argillaceous rocks. *International Journal of Rock Mechanics and Mining Sciences*. 2006, vol. 43, no. 6, pp. 950—960. DOI: 10.1016/j.ijrmms.2006.02.004.

22. Panteleev I. A., Plekhov O. A., Naimark O. B., Evseev A. V., Pankov I. L., Asanov V. A. Features of strain localization in sylvinite under tension. *PNRPU Mechanics Bulletin*. 2015, no. 2, pp. 127—138. [In Russ]. DOI: 10.15593/perm.mech/2015.2.08.

23. Ermashov A. O. *Geomekhanicheskoe obosnovanie raschetov osedaniya zemnoy poverkhnosti pri dobyche kaliyno-magnievykh rud (na primere Verkhnekamskogo mestorozhdeniya kaliyno-magnievykh soley)* [Geomechanical substantiation of calculations of subsidence of the earth's surface during the extraction of potassium-magnesium ores (on the example of the Verkhnekamskoye deposit of potassium-magnesium salts)], Candidate's thesis, Perm, 2015.

24. Frenelus W., Peng H., Zhang J. Creep behavior of rocks and its application to the long-term stability of deep rock tunnels. *Applied Sciences*. 2022, vol. 12, no. 17, article 8451. DOI: 10.3390/app12178451.

25. Baryakh A. A., Samodelkina N. A., Konosavsky P. K. Prevention of freshwater breakthrough into potassium mines. *Procedia Structural Integrity*. 2021, vol. 32 no. 6, pp. 17—25. DOI: 10.1016/j.prostr.2021.09.004.

26. Zhang L., Wang X. Study on nonlinear damage creep model for rocks under cyclic loading and unloading. *Advances in Materials Science and Engineering*. 2021, vol. 2021, article 5512972, pp. 1—10. DOI: 10.1155/2021/5512972.

27. Fei W., Jie L., Quanle Z., Cunbao L., Jie C., Renbo G. A triaxial creep model for salt rocks based on variable-order fractional derivative. *Mechanics of Time-Dependent Materials*. 2021, vol. 25, no. 1, pp. 101—118. DOI: 10.1007/s11043-020-09470-0.

28. Asanov V. A., Pankov I. L., Kuzminyh V. S., Morozov I. A. The methodical aspects of strength, deformation and energy characteristic determination of salt rocks under direct tensile loading of rock specimens in laboratory conditions. *PNRPU Mechanics Bulletin*. 2018, no. 4, pp. 58 – 68. [In Russ]. DOI: 10.15593/perm.mech/2018.4.05

29. Protosenya A. G., Katerov A. M. Substantiation of rheological model parameters for salt rock mass. *MIAB. Mining Inf. Anal. Bull.* 2023, no. 3, pp. 16 – 28. [In Russ]. DOI: 10.25018/0236_1493_2023_3_0_16.

30. Deng H., Zhou H., Li L. Fractional creep model of temperature-stress-time coupled damage for deep coal based on temperature-equivalent stress. *Results in Physics*. 2022, vol. 39, article 105765, pp. 1 – 12. DOI: 10.1016/j.rinp.2022.105765.

31.Taheri S. R., Pak A. Casing failure in salt rock: Numerical investigation of its causes. *Rock Mechanics and Rock Engineering*. 2020, no. 59, pp. 3903 – 3918. DOI: 10.1007/s00603-020-02161-9.

32. Kashnikov Yu. A., Ashikhmin S. G., Kukhtinskii A. E., Shustov D. V. On the relationship of crack resistance coefficients and geophysical characteristics of rocks of hydrocarbon deposits. *Journal of Mining Institute*. 2020, vol. 241, pp. 83 – 90. [In Russ]. DOI: 10.31897/PMI.2020.1.83.

33. Moghadam S. I., Taheri E., Ahmadi M., Ghoreishian Amiri S. A. Unified bounding surface model for monotonic and cyclic behaviour of clay and sand. *Acta Geotechnica*. 2022, vol. 17, no. 10, pp. 4359 – 4375. DOI: 10.1007/s11440-022-01521-9.

34. Shammazov I., Dzhemilev E., Sidorkin D. Improving the method of replacing the defective sections of main oil and gas pipelines using laser scanning data. *Applied Sciences*. 2023, vol. 13, no. 1, article 48. DOI: 10.3390/app13010048.

35. Abdelwahab A., Chishegorov D., Ivanov S., Mikhailov A. Influence of the main operational factors on the working capacity of a mining hydraulic excavator. *E3S Web of Conferences*. 2021, vol. 326, article 00007. DOI: 10.1051/e3sconf/202132600007.

ИНФОРМАЦИЯ ОБ АВТОРАХ

Беликов Артем Артурович[1] — аспирант,
e-mail: s205046@stud.spmi.ru,
ORCID ID: 0000-0001-5051-0680,
Беляков Никита Андреевич[1] — канд. техн. наук,
доцент, e-mail: Belyakov_NA@pers.spmi.ru,
ORCID ID: 0000-0002-9754-501X,
[1] Санкт-Петербургский горный университет.
Для контактов: Беликов А.А., e-mail: s205046@stud.spmi.ru.

INFORMATION ABOUT THE AUTHORS

A.A. Belikov[1], Graduate Student,
e-mail: s205046@stud.spmi.ru,
ORCID ID: 0000-0001-5051-0680,
N.A. Belyakov[1], Cand. Sci. (Eng.), Assistant Professor,
e-mail: Belyakov_NA@pers.spmi.ru,
ORCID ID: 0000-0002-9754-501X,
[1] Saint-Petersburg Mining University,
199106, Saint-Petersburg, Russia.
Corresponding author: A.A. Belikov, e-mail: s205046@stud.spmi.ru.

Получена редакцией 23.12.2022; получена после рецензии 20.02.2023; принята к печати 10.03.2023.
Received by the editors 23.12.2022; received after the review 20.02.2023; accepted for printing 10.03.2023.